

## **B. Warm Forming of Aluminum II**

*Principal Investigator: Ken Oikarinen*

*DaimlerChrysler Corporation*

*2730 Research Drive*

*Rochester Hills, MI 48309*

*(248) 838-5221; fax: 248-838-5300; e-mail: kco3@daimlerchrysler.com*

*Principal Investigator: Peter Friedman*

*Ford Motor Company*

*Ford Research Laboratory*

*P.O. Box 2053, MD 3135/SRL*

*2101 Village Road*

*Dearborn, MI 48121-2053*

*(313) 248-3362; fax: (313) 390-0514; e-mail: pfriedma@ford.com*

*Principal Investigator: Paul Krajewski*

*General Motors Corporation*

*GM, R&D and Planning*

*Mail Code 480-106-212*

*30500 Mound Road*

*Warren, MI 48090-9055*

*(586) 986-8696; fax: (586) 986-9204; e-mail: paul.e.krajewski@gm.com*

*Project Administrator: Constance J. S. Philips*

*National Center for Manufacturing Sciences*

*3025 Boardwalk*

*Ann Arbor, MI 48108-3266*

*(734) 995-7051; fax: (734) 995-1150; e-mail: conniep@ncms.org*

*Technology Area Development Manager: Joseph A. Carpenter*

*(202) 586-1022; fax: (202) 586-1600; e-mail: joseph.carpenter@ee.doe.gov*

*Field Technical Manager: Philip S. Sklad*

*(865) 574-5069; fax: (865) 576-4963; e-mail: skladps@ornl.gov*

---

*Contractor: U.S. Automotive Materials Partnership*

*Contract No.: FC26-02OR22910*

---

### **Objective**

- Develop and demonstrate a production process for the warm forming (WF) of aluminum for automotive body structures and measure the economic feasibility of the WF process in a mass production environment.

### **Approach**

- Develop individual elements of the WF process in a laboratory environment, including alloy characterization, lubricant development, and process thermal modeling.
- Develop full-size demonstration of WF process and run tests in a production environment. Integrate a blank preheater, blank transfer mechanism, lubricant application system, WF press with a modified thermal profile

controller, and lubricant removal step into production trials. Conduct production feasibility tests of the warm forming process at standard rates for current forming processes.

- Create a technical cost model that can generate cost comparisons between a warm-formed aluminum door inner and a same or similar door inner manufactured using conventional forming processes in steel and aluminum.
- Expect significant improvements in the formability of aluminum to be achieved through development of enabling WF process advancements, including:
  - Establishing the degree of improvement in formability of production-grade, commercial aluminum alloys.
  - Developing a cleanable lubricant suitable for use in a WF process.
  - Optimizing the temperature distribution of the die for improved thermal control and formability.
  - Evaluating rapid preheating systems for blanks.
  - Optimizing the process design and layout.
  - Applying the results of the cost model to optimize process design.
- Demonstrate the manufacturing feasibility and economic feasibility for a new mass production process such as the WF process, by defining the process flow and developing and applying a technical cost model that allows comparison of a product made in the WF process with a comparable component fabricated from aluminum/steel with deep draw using current processes.

## Accomplishments

- Completed aluminum alloy characterization and laboratory-based WF process studies, including aluminum alloy sheet fabricated from custom-formulated 5000 series alloys and commercial alloys 5182-O, 5182-H18, 5754-O, and 5754-H18.
- Identified a suitable lubricant through extensive laboratory-based studies.
- Continued progress in the thermal analysis of the die through heat transfer analyses of the WF dies to be used in the WF process scale-up.

## Future Direction

- Complete thermal studies and thermal models for finite-element analysis (FEA) for die heater optimization.
- Fabricate blank heating system to be used in production demonstration.
- Finish die refurbishment, and prepare it for use in production scale-up.
- Set up and conduct production scale-up and demonstration, and perform coupon evaluations.
- Employ the technical cost model to compare costs of WF process and alternative processes.

## Introduction

The need to improve fuel economy has led automakers to explore lightweight materials such as aluminum for automobile body and closures. While attractive from a mass perspective, there are many challenges to the widespread use of aluminum:

- limited formability compared to steel,
- sliver management in trimming aluminum panels, and
- appearance problems in most 5000-series

aluminum panels.

The Warm Forming of Aluminum, Phase II, project was initiated after the initial technical feasibility of forming complex shapes at elevated temperatures was previously demonstrated in Phase I. It is a 4-year development and demonstration program to establish the “production” feasibility of warm forming (WF) aluminum alloy blanks into automotive panels and to fully demonstrate a WF

process for cost-effectively manufacturing aluminum automotive panels that require a deep drawn shape.

This project focuses on the following objectives:

- Developing and demonstrating a WF process, including the materials, equipment, and heating processes that can cost-effectively expand the forming limits of aluminum sheet.
- Developing a technical cost model for the WF process to evaluate the economic feasibility of the WF process specific to component design.

The key enabling process improvements to make WF a production-capable process are the following:

- A high-temperature lubricant with good lubricity at WF conditions and preferably which is easy to clean prior to automotive painting.
- Temperature distribution management on the die surface during the forming operation.
- Effective preheating method for blanks.
- Identifying an optimum alloy for WF and characterizing its mechanical behavior at elevated temperatures.

## **Phase II Detail**

**Technical Cost Model:** Camano Associates developed a detailed cost model based on a process sequence defined by the project team. Through use of the cost model, it was identified that aluminum alloy cost accounted for more than 70% of the cost of the end product. Thus, project research was re-focused on commercially available alloys rather than “new” alloys with exotic alloying additions.

**Alloy Selection:** The University of Michigan completed analyses of the warm formability of commercial aluminum alloys and identified parameters affecting the sheet fabrication process for WF-capable aluminum sheet.

**Lubricant Selection:** The performance of selected lubricants under various temperature, travel time, and load pressures was evaluated at the University of Michigan in collaboration with General Motors (GM) and Fuchs’ Lubricants.

**Die Thermal Analyses:** University of Michigan’s S. Wu Manufacturing Center performed finite-element analyses of temperature profiles on the WF tooling for Neon door inners. Die geometry and heater location data were obtained from computer-aided design (CAD) models provided by Sekely Industries.

**Blank Heating:** Evaluations of infrared (IR) heating and a conduction heating methodology for heating laboratory-scale blanks were investigated at The University of Michigan and Ford Motor Company, respectively. The results assisted the team in selecting the preferred heating methodology for blank preheating for a WF production process.

**Alloy Fabrication:** Pechiney Rolled Products supplied the specified 5000 series aluminum sheet for these formability studies.

**Full-scale Process Demonstration:** With the individual component processes validated at laboratory level for technical and economic process feasibility, the full-scale WF demonstration using the Dodge Neon door inner stamping dies will be conducted starting in mid-2005. The process demonstration may be conducted in the local Detroit area, subject to acceptable vendor proposed terms.

**Postprocess inspection and material analyses:** Coupons from warm-formed parts will be cut out, and the materials properties will be evaluated by one of the original equipment manufacturers (OEMs). The typical properties to be evaluated will include strength, distortion, and corrosion.

## **Phase II Accomplishments**

### **Alloy Characterization**

This work was performed on Pechiney’s Al-Mg alloys: 5182-O, 5182-H18, 5754-O and 5754-H18. Optical microscopy was performed at The University of Michigan. Cross-sectional photomicrographs of the 1-mm sheet alloys in the rolling-thickness planes are shown in Figure 1. The 5182-O alloy shows nearly equiaxed, annealed grains of average size of 7–9  $\mu\text{m}$ , and the heavily rolled 5182-H18 alloy shows elongated grains that are 22  $\mu\text{m}$  long and 2.6- $\mu\text{m}$  average thicknesses. During polishing of the samples, second phase, coarse particles containing silicon, iron, and intermetallics fall off, leaving small pores; but in the H18 alloy, several particles, 15- to 20- $\mu\text{m}$  size, are found severely damaged, and the matrix surrounding those particles severely deformed and cracked. From this information, it is understandable that formability of H18

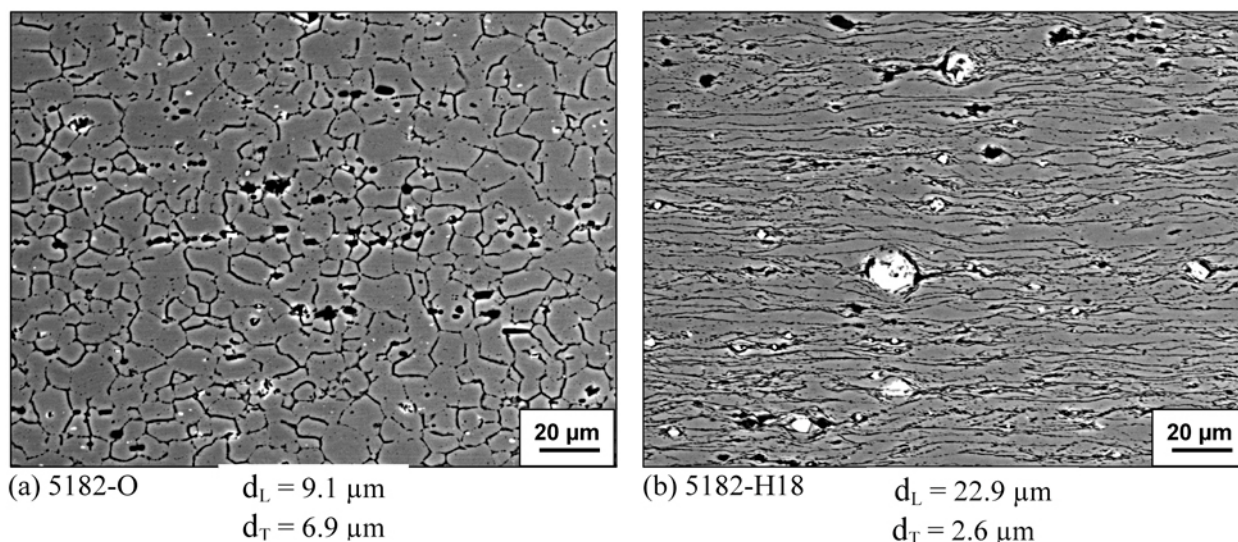


**Figure 1.** Microstructure of Pechiney alloys showing nearly equiaxed grain structure in the O-condition and elongated grains in the H-18 condition.

alloy would be severely impaired without a proper recrystallization and damage healing treatment. Alternatively, cleaner alloys with less content of large particles would be desirable. 5754-O and 5754-H18 alloys showed similar microstructures, but contained fewer particles.

### Blank Preheating and Forming Studies

Blank preheating and forming studies were completed by the University of Michigan. A small laboratory-size IR heating oven (660 mm in length), manufactured by IR Heating Technologies, Inc., of Oak Ridge, Tennessee, was used to heat the sheets and convey them to the preheated laboratory cup-forming test machine. The IR heating equipment has a stainless steel chain belt system, driven by a variable-speed motor. The equipment did not come with a variable-speed control, which was subsequently installed by the University. Total IR heating power was approximately 20–24 kW, but the heating lamps were approximately 150 mm from the surface of the aluminum sheets, which minimized power coupling. The heat loss from the inlet and exit of the heater was significant. Insulation at the entry and exit was added to contain the heat within the furnace so that the IR lamps could effectively heat the sheet (blank).

The following experiments were conducted to determine the attributes of the IR heater capability and its effect on heating time, including the degree

of recrystallization and forming performance of aluminum sheets:

1. effect of belt speed and temperature setting to reach various constant temperatures in the hot zone of the furnace;
2. the rate of temperature rise and exit temperature during passage of the sheet through the oven;
3. minimum time to reach 350°C exit temperature;
4. possibility of raising the sheet closer to the IR heating lamps;
5. degree of recrystallization of the alloys achieved upon exit from oven;
6. effect of preheating on the height of the formed cup;
7. role of lubricants, such as moly-disulfide, boron nitride, and Fuchs lubricants on cup height at fracture; and
8. cup height measurements on 5182-O, 5182-H18, 5754-O, 5754-H18, and also Alloy 725 used from an earlier WF study.

A variable-frequency potentiometer control was installed to drive the chain belt over a wide range of speeds with a maximum speed capability of 60 mm/s. A linear behavior between input power frequencies vs conveyor speeds is shown in the curves in Figure 2. Sheet samples were connected with thermocouples and traveled through the oven at various speeds at different temperature settings. It was anticipated that reaching a constant temperature

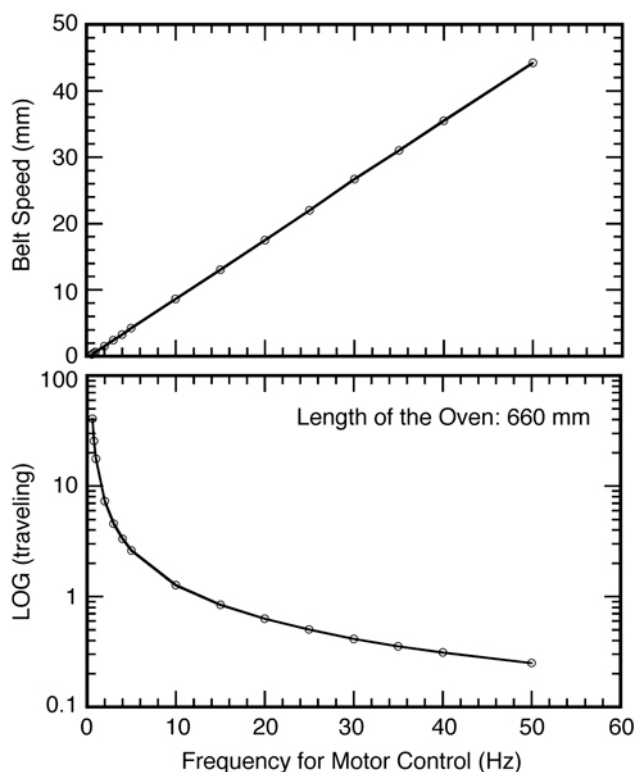


**Figure 2.** Belt speed control as a function of motor frequency and corresponding traveling time.

profile within the oven was desirable to achieve uniform temperature over a period of time needed to anneal and recrystallize the hard temper aluminum sheets. However, for oxygen-temper sheets, the recrystallization step is not deemed necessary, and rapidly heating the sheet for minimizing forming time was needed. Initial experiments were performed at a 400°C furnace setting with a view to attain a constant temperature in the range of 350–400°C. Figure 3 shows temperature rise as a function of time of travel through the oven. These trials with the IR heater showed the time to heat the blank to 300°C was approximately 3 min at an oven temperature of 400°C.

The next series of experiments were performed with IR heater settings at 800–900°C to accelerate heating of blanks at rapid rates. A series of experiments was performed with specimens attached with thermocouples, each with a different conveyor speed such that the entry-to-exit time could be monitored. These experiments were performed to understand the general characteristics of these ovens and to examine alternative strategies where total residence

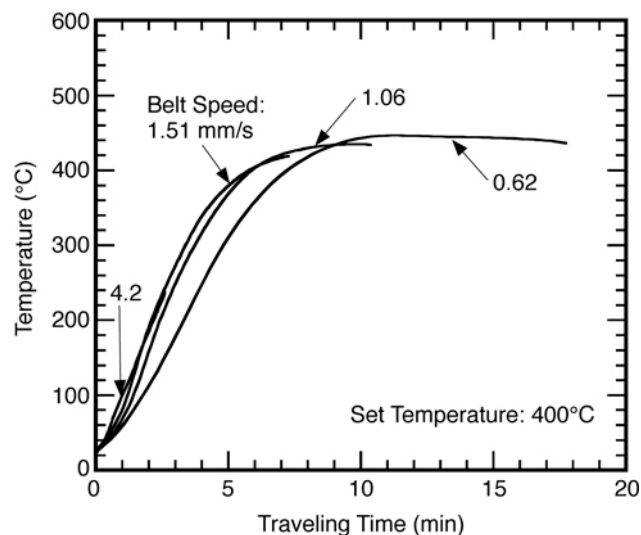


**Figure 3.** Sheet temperature as a function of time for three different belt speeds at an oven set temperature of 400°C.

time in the oven could be longer without compromising sheet exit rate. The rise in sheet temperature with various exit times is shown in Figures 4 and 5, with corresponding microstructural changes. Recrystallization effects are seen when the heavily deformed H18 microstructure is replaced by equiaxed grains.

Time to reach 300°C for these trials was closer to 35 and 25 s at 800°C and 900°C temperatures, respectively. This represents a significant improvement over the previous results at a set temperature of 400°C.

Recrystallization prior to forming is required to attain maximum formability. Material cost savings can be attained by using "hardened sheet" such as these instead of having the sheet batch-annealed at the aluminum manufacturing facility. However, for oxygen-temper sheets, a recrystallization step is not deemed necessary and rapid heating of the sheet was needed to minimize forming time.

While these trials demonstrated that an IR oven is capable of supplying ample heating for the WF process, it did not appear to be the best solution. Significant overheating appears to be necessary to achieve production feasible heat-up times. Additionally, overheating presents the risk of melting the sheet if the conveyor system were to stop for any period of time. Additionally, high emissivity of aluminum requires significant energy from the IR

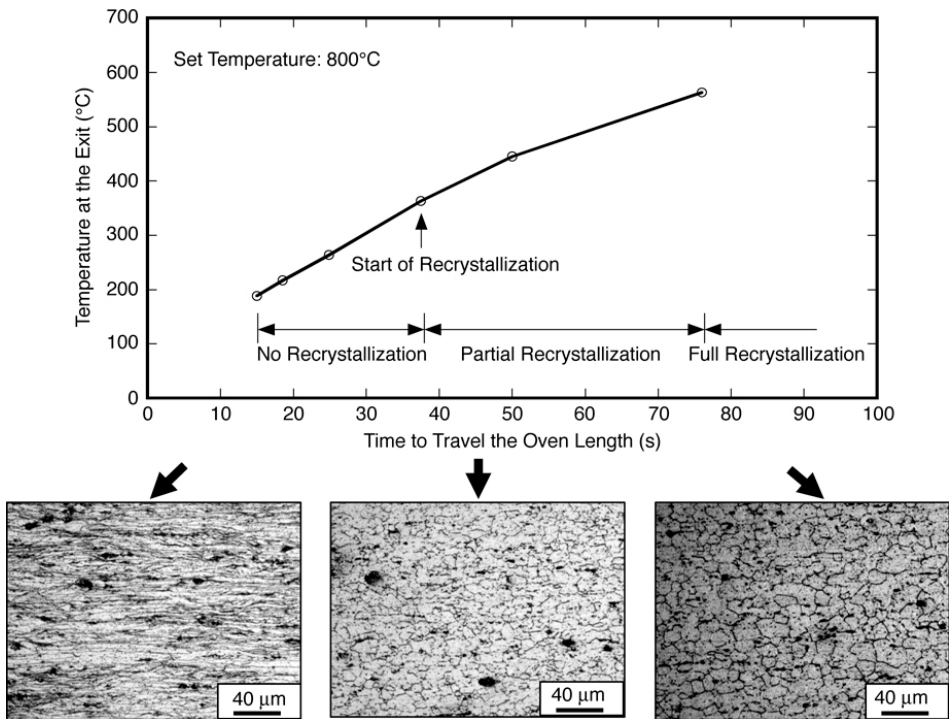


**Figure 4.** Heating and recrystallization of 5182-H18 alloy during passage through IR oven for various conveyor speeds (set temperature 800°C).

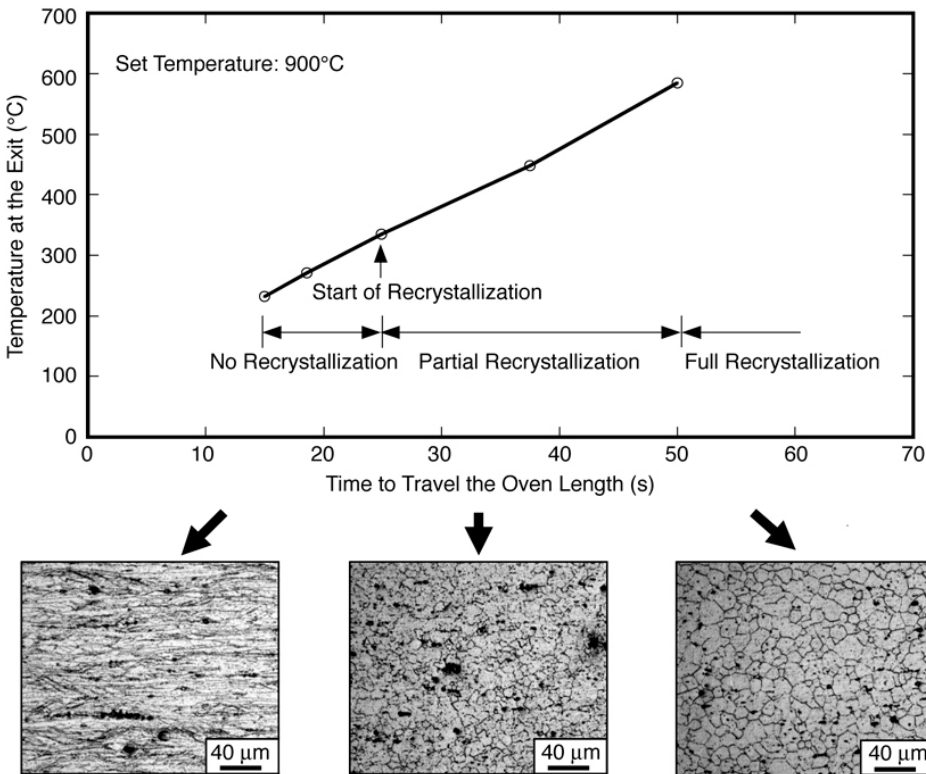


**Figure 5.** Heating and recrystallization of 5182-H18 alloy during passage through IR oven for various conveyor speeds (set temperature 900°C).



heater to reach target temperatures. For these reasons, the team decided to use a conduction heater in the scale-up of the WF process, which is thought to be a more cost-effective and robust method of heating aluminum sheet. Preliminary tests indicate that forming temperatures can be reached within seconds with this type of heater.

### **Biaxial Forming Tests, Forming Limit Measurement, and Lubricant Studies**

Forming tests were performed on a heated rectangular die-punch apparatus designed and built at the University of Michigan, to simulate commonly observed biaxially formed parts and appropriate punch and die edge radii. Figure 6 shows a schematic diagram of the main part of the WF test device and a photograph of the die-punch configuration. Sheet blank size used in this work was 200 mm by 140 mm. Die opening area was approximately 110 mm by 50 mm including the die entry radius, and the overall punch size was 100 mm by 40 mm. Both the die edge and the punch had edge radii of  $\sim 5$  mm.

The die and the punch were heated by embedded heating elements. Thermocouples inserted into different heating areas of the die and the punch

permitted temperature control using proportional integral derivative (PID) devices, within a range of  $\pm 4^\circ\text{C}$ . The punch-die device was mounted on an Instron-1116 testing machine with 250-kN capacity. The punch was actuated by moving the machine crosshead at predetermined speeds. The upper die plate was maintained in a fixed position in the die apparatus, while the lower die plate was moved upward by using the pistons of three ENERPAC hydraulic cylinders to clamp the sheet between them. The die and punch were preheated to desired temperature(s) and then the preheated sheet sample was moved into position marked on the lower die where a specified blank holding load (average pressure of 1.1 MPa) was applied to tightly clamp the sheet. The forming test temperature range was selected to be  $\sim 350^\circ\text{C}$ , and room temperature tests were used as baseline references.

It was found that thermal equilibrium could be reached in just a few seconds. The punch advance speed was fixed at 10 mm/s, providing local strain rates in the small test sample close to commercial stamping strain rate. Load vs punch displacement curves were recorded using an X-Y data recorder, and the data were utilized to obtain the depth of a

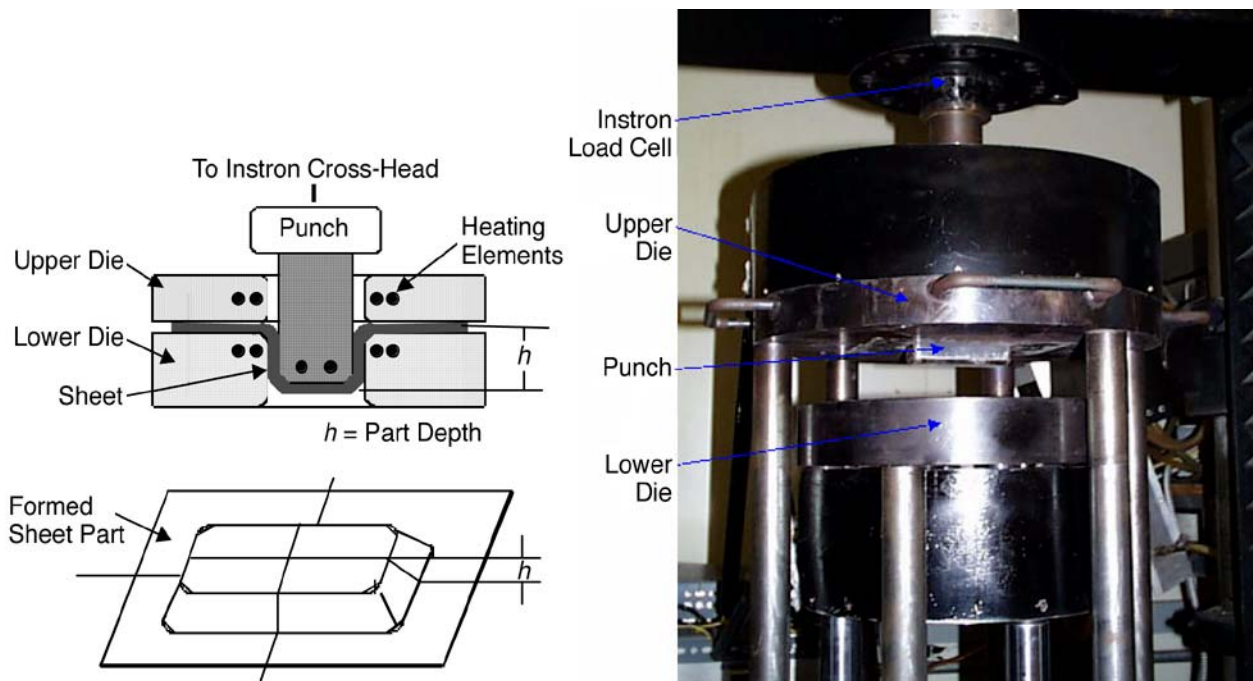


**Figure 6.** Schematic diagram of the main parts of the WF test device and a formed blank, and photograph of the rectangular die-punch apparatus with heated die set.

formed part at peak load (where necking occurred in the sheet). This part depth was used as the measure of formability.

To evaluate forming strain and to construct forming-limit diagrams (FLDs), the preetched grid size was measured using a video camera and digitally processed by a computer program (Scion Image) for the warm-formed rectangular parts. The measurements were made along both longitudinal and transverse axes and around the crack. Different lubrication and different blank holding pressure were utilized to permit failure in different regions of the formed cups such that the state of strain at failure could be altered, a requirement for determining the forming limit diagram. Grid strains were utilized for determining the FLD by using established techniques. The FLD of 5182-O aluminum was found to be lower in level compared to fine grain alloy 5182 + Mn and 5754 alloys studied previously during an earlier phase of the WF project (see website <http://www.mse.engin.umich.edu/research/groups/ghosh/>), also supported by the Department of Energy.

The effectiveness of lubrication was determined by measuring cup height from samples coated with different lubricants. In addition to spray coatings of boron nitride and molybdenum sulfide, synthetic lubricants supplied by Fuchs Lubricants were evaluated. The latter lubricants were evaluated in their "pure" state as well as after the addition of small levels of BN and MoS<sub>2</sub>. Figures 7–9 shows cup heights at failure of samples tested with the various lubricants, under the same nominal test conditions.

In general, moly-disulfide lubrication produced equal or slightly inferior cup height in comparison to BN-coated samples, with values in the range of 18–21 mm. The Fuchs lubricant 216 gave the best performance when it contained some BN or moly-disulfide. The 216-BN was found to be the best lubricant, exhibiting a cup height of 25 mm. Without BN, the 216 lubricant was inferior to solid lubricants BN and moly-disulfide by themselves. A typical problem encountered with the use of Fuchs 216-based lubricants was a heavy, tenacious brown stain formation on the cup surface due to curing of the polymer base and bonding to aluminum.

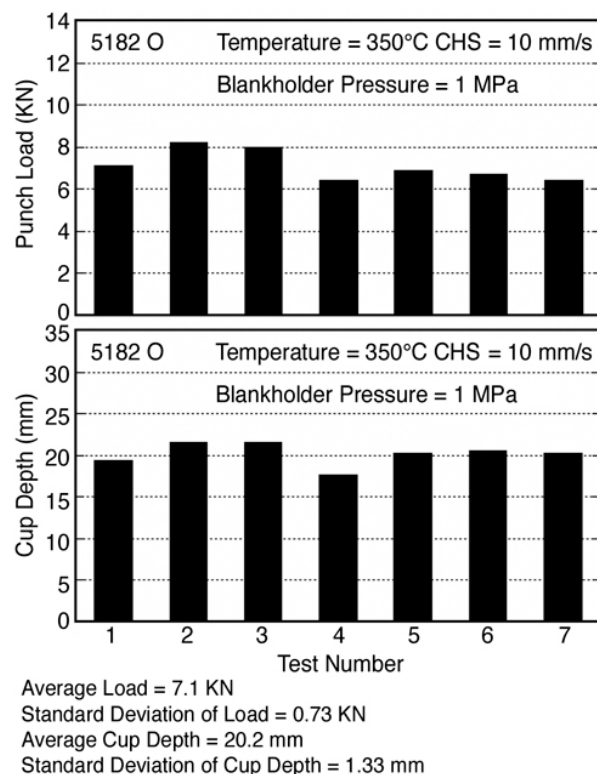


**Figure 7.** Variability in punch load and cup height, using moly-disulfide lubrication on 5182-O aluminum alloy.

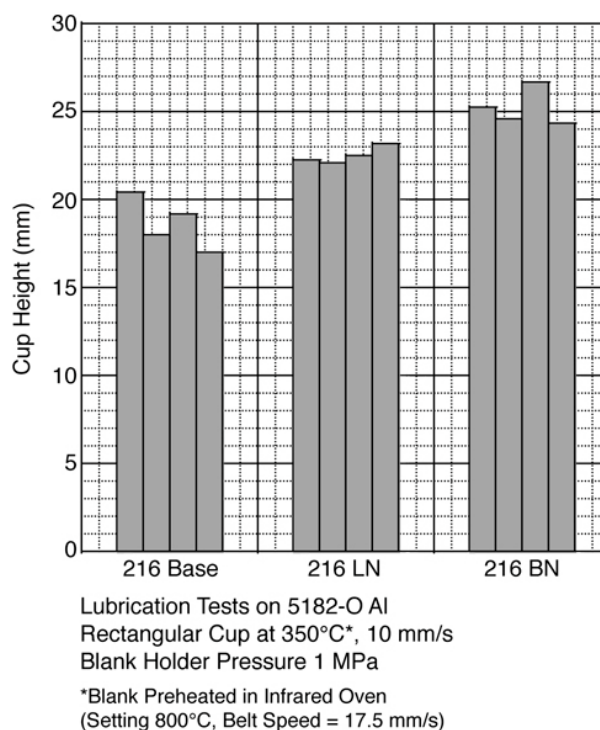


**Figure 8.** Cup height data, using various lubricants supplied by Fuchs Lubricants.



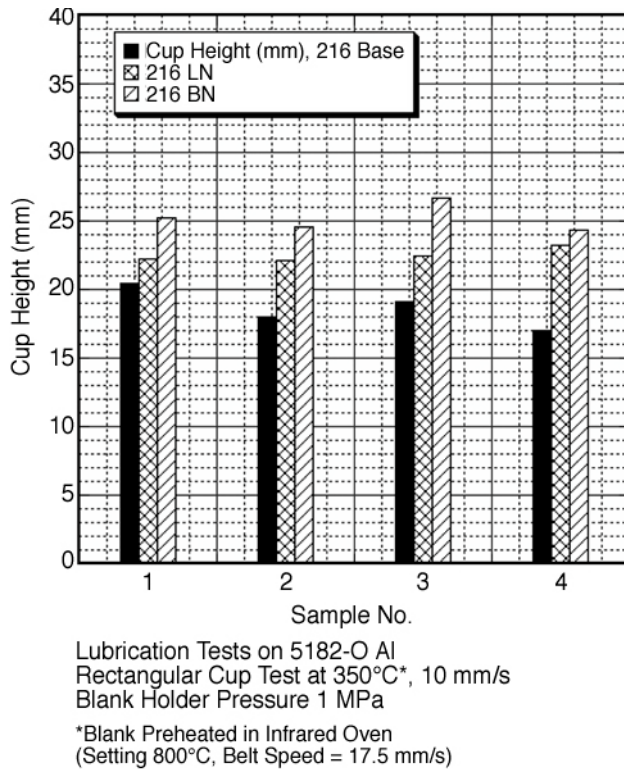


**Figure 9.** Data similar to that in Figure 8, showing superiority of lubricants containing small amount of BN over the base lubricant.

### **Tensile Deformation Behavior of 5182-O Aluminum Alloy after Preheating in an IR Heating Oven**

Uniaxial tensile deformation behavior of 5182-O aluminum sheet alloy after preheating was studied in the temperature range from room temperature to 350°C and in the strain rate range of 0.015–1.33 s<sup>-1</sup>. Strain rate, the relationship between stress and temperature, was studied. The total elongation in uniaxial tension is found to increase with increasing test temperature and to decrease with increasing test strain rates. The strain rate sensitivity (*m* value) is determined for the data produced at different strain rates. Also, the recovery effect during the tension test was investigated at different temperatures and strain rates based on the stress-strain curves obtained in the uniaxial tension test. It was found that total dynamic recovery effect in uniaxial tension increases with increasing temperature and decreases with increasing strain rate.

Findings from these studies include:

- **Stress-strain relations**—The tensile load-displacement data were processed to obtain true stress-true strain data. True stress-true plastic strain curves were obtained at four temperatures (25, 250, 300, and 350°C) and at three strain rates (0.015, 0.15, and 1.33 s<sup>-1</sup>). Engineering stress-strain curves were obtained for the material at different strain rates and temperatures. For 5182-O aluminum sheet alloy, flow stress level increases with increasing strain rate but decreases with increasing temperature.
- **Tensile elongation**—In general, total elongation increases with increasing temperature and decreases with increasing strain rate. The enhanced total elongation becomes significant only above 250°C. Thus, 250°C appears to be the lower end of the WF temperature range. Tensile elongations in the range of 60–110% were achieved at 350°C. For strain to the maximum load, that is, uniform elongation, it was observed that the variation of uniform elongation does not follow a single trend against temperature or strain rate. In fact the value of uniform elongation actually increases with increasing temperature in some of the 5xxx alloys. Thus, the combined influence of temperature and strain rate may be complex.
- **Strain rate sensitivity of flow stress**—The strain rate sensitivity index of flow stress, *m*, is determined according to

$$m = d(\log \sigma)/d(\log \dot{\epsilon}) \quad (1)$$

where  $\dot{\epsilon}$  = strain rate. The value of *m* is an important material property in evaluating the formability of a sheet metal. Currently, there are different test methods to determine *m* value. The present tensile tests provided data of true stress-true plastic strain relations at each temperature. The *m* value is then calculated according to Eq. (1). The log  $\sigma$ -log  $\dot{\epsilon}$  relationships at different temperatures based on peak stress level (steady state) for each test were plotted, and the values of *m* were determined from the slopes of the curves. These *m* values are then plotted against temperature. It is found that *m* value increases markedly with increasing temperature. It is zero

at room temperature, 0.044 at 250°C, 0.099 at 300°C and 0.15 at 350°C. The reason for this is that at higher temperature atoms move more rapidly, and dislocation climb becomes easier. Climb and thermally activated glide lead to a higher  $m$  value with increasing temperature. We also can see that, the  $m$  value is not very high, for example, it is 0.15 at 350°C. The relatively low value of  $m$  indicates that the mixture of thermally activated glide and climb is the dominant deformation mechanism for 5182-O aluminum alloy. As for pure climb, the  $m$  value should be substantially higher, while for thermally activated glide, the  $m$  value is generally below 0.1. Because the higher value of  $m$  indicates larger elongation, the elongation will increase with the increasing temperature.

- Dynamic Recovery Effect—During the warm deformation process, two competing effects, strain hardening and dynamic recovery occur, leading to the attainment of a steady flow stress. On one hand, as the specimen is elongated, the dislocations in the material interact with each other and become tangled leading to a reduced effective distance between these obstacles, thereby increasing the resistance to the movement of subsequent dislocations. As a result, higher stress is needed to deform the specimen further.

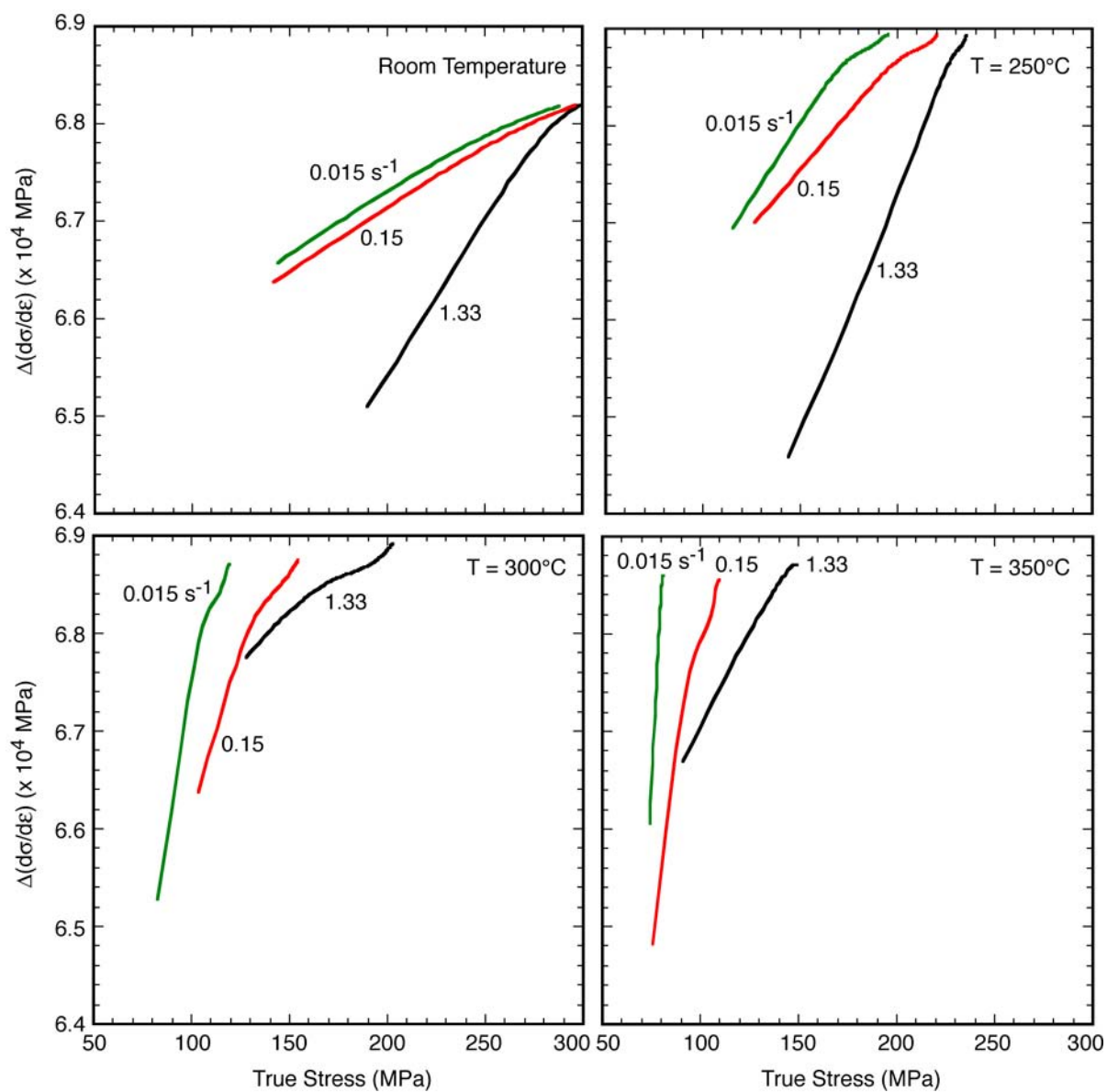
In contrast, because the specimen is deformed at elevated temperature, recovery and rearrangement of dislocations occur concurrently due to their greater mobility and annihilation of each other, therefore minimizing the stored dislocation density and increasing the spacing between the dislocations, thereby reducing deformation resistance. Reduced obstacle density tends to lower the flow stress leading to an equilibrium dislocation structure, and a steady state flow stress. Net hardening was found to increase with increasing strain rate, indicating that softening due to dynamic recovery is reduced at higher strain rates. Consequently, strain to maximum load increases as strain rate increases. The fact that uniform strain increases with increasing strain rate is a clear indication that dynamic recovery or softening is reduced at higher strain rates.

The tendency for dynamic recovery is a critical indicator for warm formability and for the measured  $m$  values. To investigate the recovery effect due to temperature and strain rate, a method to quantify its extent was devised. For the tests, the change in the slope of the stress-strain curve,  $\Delta(d\sigma/d\epsilon)$ , was compared to that at room temperature as a measure of recovery effect (at given values of flow stress, the state parameter for stored structure, and its deformation resistance). We define  $\Delta(d\sigma/d\epsilon)$  as the recovery parameter  $R$ . To determine the value of  $R$ , the reference value is either the elastic or the plastic slope: in this case, the Young's modulus  $E$  of 5182-O aluminum alloy at room temperature,  $S_1 = 69,000$  MPa, and  $S_2$ , the slope of true stress-true strain curve at an elevated temperature at a specific stress level ( $R = S_1 - S_2$ ).

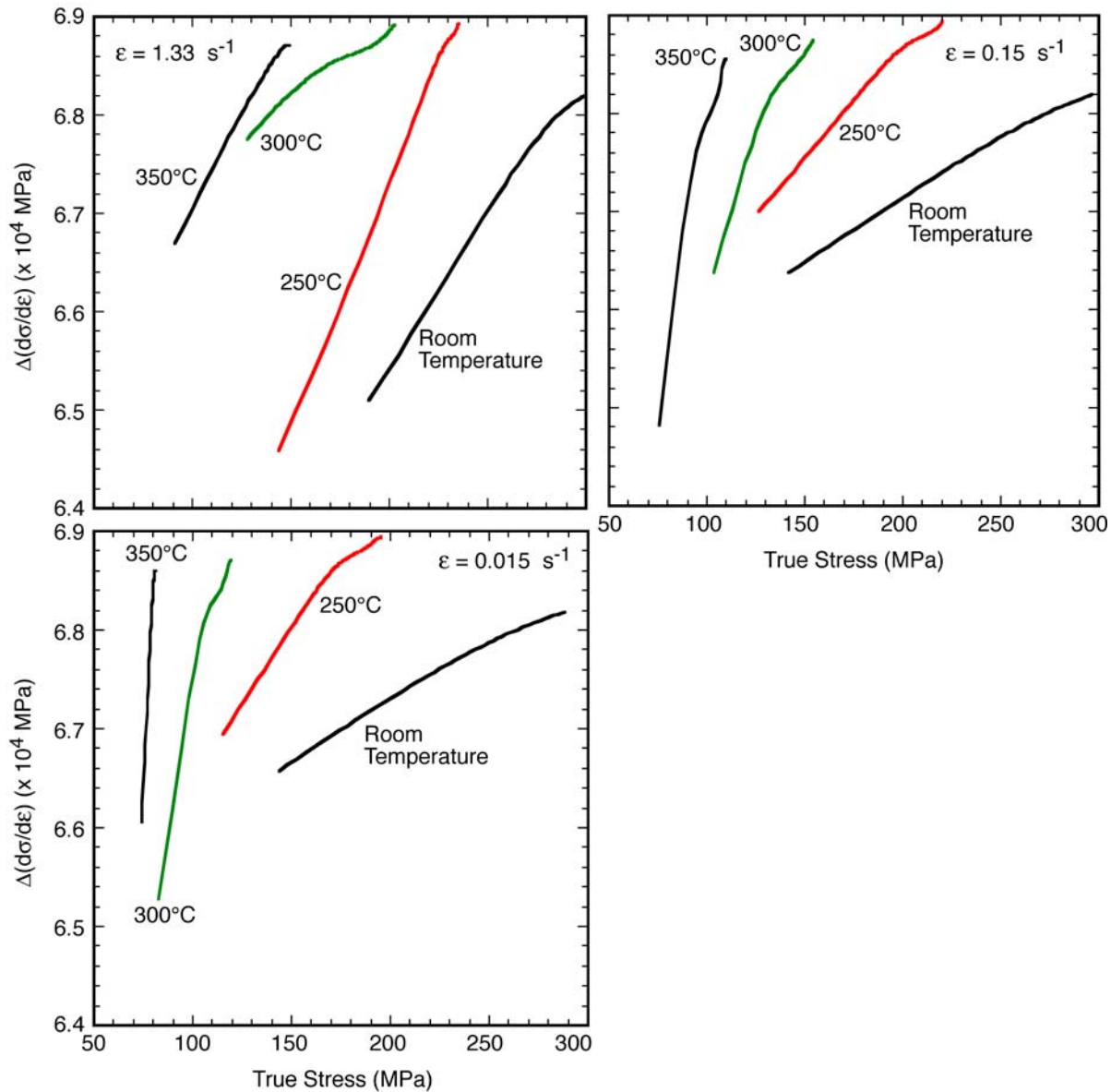
Figure 10 shows  $\Delta(d\sigma/d\epsilon)$  as a function of true stress at different strain rates at specific temperatures. The recovery effect increases with the increasing true stress level, because higher stored dislocation density drives faster recovery. Also at a specific stress level, the recovery effect increases with the decreasing strain rate. The reason for this is that at a lower strain rate, more time is available for dislocations to annihilate each other and more time is available for recovery. Thus, recovery effect is much more obvious at lower strain rate.

Figure 11 shows  $\Delta(d\sigma/d\epsilon)$  as a function of true stress at different temperatures at a specific strain rate. At a specific stress level, the recovery effect increases with the increasing temperature. The reason for this is that at higher temperature, atomic transport is more rapid. Furthermore, faster deformation rates minimize the time available for dislocation annihilation and rearrangement. This reduces the degree of softening achievable by recovery.

For the 5182-O aluminum sheet alloys studied in the WF temperature range of 200–350°C and in



**Figure 10.** Recovery effect at different temperatures for 5182-O aluminum based on tensile test.



**Figure 11.** Recovery effect at different strain rates for 5182-O aluminum based on tensile test.

the strain rate range of  $0.015\text{--}1.33 \text{ s}^{-1}$ , the following conclusions can be drawn:

- Uniaxial tensile elongation increases with increasing temperature and decreases with increasing strain rate. The maximum tensile elongation observed ranged between 60–100% at 350°C.
- Strain rate sensitivity ( $m$  value) increases with increasing temperature, and the strain hardening rate increases with increasing strain rate in keeping with dynamic recovery effects. Strain rate hardening is deemed to play a dominant role

in enhancing the elevated temperature plasticity in tensile deformation.

- Dynamic recovery effect [ $\Delta(d\sigma/d\epsilon)$  value] increases with increasing stress level. And at a specific stress level, the total amount of recovery effect increases with increasing temperature and/or decreasing strain rate.

### **Die And Blank Thermal Analyses**

Positive progress was made during 2004 in the thermal analysis of the WF dies through a heat transfer analysis of the dies to be used in the WF

process scale-up. A preliminary finite-element analysis (FEA) model to study the heatup and cooling of formed parts and die components was defined by S. M. Wu Manufacturing Research Center, University of Michigan. The FEA model was then used to examine the effects of air vs water cooling on simple deep draw parts, the loss of temperature during sheet material transfer from preheater to die, and heat distortion effects on die and insert surfaces over time. Such information will be considered in the final process layout design.

Six parts (insert, lower holder, blank, upper holder, punch, and base) make up this complex die-punch process.

- In early simulations, heat fluctuation values for the die upper and lower holders, insert and punch were analyzed with and without a heater control scheme. Findings at that time concluded that desired steady state temperature values (350°C) can be achieved in significantly shorter time by using a heater control scheme. Additionally, steady state temperature can be maintained precisely through the use of a heater control scheme.
- The WF cycle was simulated using a sectional model. Findings indicate that the change in temperature of the upper and lower rings, insert and punch during a single forming cycle is negligible ( $\pm 3^\circ\text{C}$ ).
- FEA with the heater control scheme on actual tooling was performed on the lower tooling, insert, and lower ring. Simplification of the models was done to reduce the model size and computational time. For example, the modified model for the insert reduced the number of nodes from 60,375 with 38,775 elements to 42,654 with 26,699 elements. Comparison of FEA and experimental results yielded these conclusions:
  - Using constant heat flux values, time to reach steady state temperature of 350°C takes 25 h and 10 h for the insert and lower ring, respectively.
  - Using the heater control scheme can reduce the time to reach steady state to ~2 h.
  - Vertical displacement distribution ranges from 0.68 to 0.8 mm in the insert, and 0.6 to 1.25 mm in lower ring.

Future work will complete FEA of the upper tooling with the heater control scheme and will verify FEA results against actual thermal data from the demonstration experiments. These data will then be incorporated into an FEA for determining optimal heater specifications for future tooling/process design.

## **Summary and Conclusions**

**Alloy Selection:** 5182-O aluminum alloy has sufficient attributes for WF to support its use in the scale-up demonstration phase. Findings from the alloy characterization studies pertinent to the scale-up demonstration phase include the following:

- Full hard 5182 aluminum has observable rolling-induced damage, which is absent in 5182-O.
- Full hard 5182 alloy can be recrystallized by rapid heating; formability remains worse than 5182-O sheet.
- 5182-O alloy shows a cup height of 20 mm at 350°C.
- 5182-O alloy has a biaxial forming limit of 40% by 40% (approximately) at 350°C.

In the demonstration phase, magnesium sheet will be tested using the WF demonstration process and tooling to empirically evaluate the result. Magnesium behavior and blank forming results will help the OEMs determine what developmental work may be required to form magnesium.

### **Blank Preheating and Forming Studies:**

While our lab trials demonstrated that an IR oven is capable of supplying ample heating for the WF process, it does not appear to be the best solution. Significant IR lamp overheating appears to be necessary to achieve production-feasible heat-up times. Additionally, overheating presents the risk of melting the sheet if the conveyer system were to stop for any period of time. For these reasons, the team decided to fabricate a conduction heater for use in the scale-up of the WF process. It is thought to be a cost-effective and robust method of heating aluminum sheet. Preliminary tests indicate that forming temperatures can be reached within cycle time requirements.

In general, moly-disulfide lubrication produced equal or slightly inferior cup height in comparison to BN-coated samples, with values in the range of 18–21 mm. The Fuchs Lubricants 216 wax-based



varieties with BN or moly-disulfide produced the best results. 216-BN was found to be the best lubricant exhibiting a cup height of 25 mm. Because it is a wax-based lubricant, a heavy, tenacious brown stain forms on the cup surface due to curing of the polymer base and bonding to aluminum. Future work may consider development of economical cleaning solutions for this lubricant.

For the 5182-O aluminum sheet alloys studied in the WF temperature range of 200–350°C and in the strain rate range of 0.015–1.33 s<sup>-1</sup>, the following conclusions can be drawn:

- Uniaxial tensile elongation increases with increasing temperature and decreases with increasing strain rate. The maximum tensile elongation observed ranged between 60–100% at 350°C.
- Strain rate sensitivity increases with increasing temperature, and the strain hardening rate increases with increasing strain rate in keeping with dynamic recovery effects. Strain rate hardening is deemed to play a dominant role in enhancing the elevated temperature plasticity in tensile deformation.

- Dynamic recovery effect increases with increasing stress level. And at a specific stress level, the total amount of recovery effect increases with increasing temperature and/or decreasing strain rate.

**Lubricant Studies:** Fuchs lubricant 216 BN produced the best cup height of all formulations studied, exhibiting a cup height of ~25 mm, and appears to be a feasible lubricant for use in the scale-up demonstration. Cleaning options and methodologies will be defined during the demonstration stage.

**Die and Blank Thermal Analyses:** Modeling performed to date represents positive progress toward development of an FEA for determining optimal heater specifications for future tooling/process design. Future work on this task will complete FEA of the upper tooling with heater control scheme and will verify FEA results against actual thermal data from the demonstration experiments. These data will then be incorporated into an FEA for determining optimal heater specifications for future tooling/process design.